Applied Microbiology and Biotechnology (2022) 106:5105–5121
https://doi.org/10.1007/s00253-022-12034-6

APPLIED GENETICS AND MOLECULAR BIOTECHNOLOGY

Dynamic control of 4-hydroxyisoleucine biosynthesis by multi-biosensor in *Corynebacterium glutamicum*

Wenmei Lai[1,2] · Feng Shi[1,2,3] · Shuyu Tan[1,2] · Haiyan Liu[1,2] · Yongfu Li[4] · Youhe Xiang[1,2]

Received: 15 January 2022 / Revised: 15 June 2022 / Accepted: 16 June 2022 / Published online: 28 June 2022

Abstract

4-hydroxyisoleucine (4-HIL) has a potential value in treating diabetes. The α-ketoglutarate (α-KG)-dependent isoleucine dioxygenase (IDO) can catalyze the hydroxylation of L-isoleucine (Ile) to form 4-HIL by consuming O_2. In our previous study, the *ido* gene was overexpressed in an Ile-producing *Corynebacterium glutamicum* strain to synthesize 4-HIL from glucose. Here, a triple-functional dynamic control system was designed to regulate the activity of IDO, the supply of α-KG, O_2, and Ile and the synthesis of by-product L-lysine (Lys) for promoting 4-HIL synthesis. Firstly, the codon-optimized *ido* was positively regulated by seven Ile biosensors Lrp-P_{brnFE}N with different intensities, and the resulting seven D-$_N$I strains produced 38.7–111.1 mM 4-HIL. Then on the basis of D-$_N$I, *odhI* and *vgb* were simultaneously regulated by three P_{brnFE}N with different intensities to synergistically control α-KG and O_2 supply. The 4-HIL titer of twelve D-$_N$I$_N$O$_N$V strains was more than 90 mM, with D-$_0$I$_7$O$_7$V generating the highest titer of 141.1 ± 15.5 mM. Thirdly, *ilvA* was negatively regulated by an Ile attenuator P_{ilvBNC} on the basis of D-$_N$I strains and some D-$_N$I$_N$O$_N$V strains to balance the synthesis and conversion of Ile. The resulting D-$_N$IPA strains produced 73.6–123.2 mM 4-HIL, while D-$_7$I$_7$O$_1$VPA accumulated 127.1 ± 20.2 mM 4-HIL. Finally, *dapA* was negatively regulated by a Lys-OFF riboswitch and Lys content decreased by approximately 70% in most D-RS-$_N$IPA strains. A strain D-RS-$_5$IPA with the highest 4-HIL titer (177.3 ± 8.9 mM) and the lowest Lys concentration (6.1 ± 0.6 mM) was successfully obtained. Therefore, dynamic regulation of main and branch pathway by three functional biosensors can effectively promote 4-HIL biosynthesis in *C. glutamicum*.

Key points

- *Three biosensors were coordinated for dynamic 4-HIL biosynthesis in C. glutamicum*
- *Bidirectional regulation of Ile synthesis and conversion promoted 4-HIL synthesis*
- *Negative regulation of Lys synthesis further increased 4-HIL production*

Keywords 4-Hydroxyisoleucine · *Corynebacterium glutamicum* · Dynamic control · *Lrp*-P_{brnFE}N · P_{ilvBNC} · Lys-OFF riboswitch

Introduction

Metabolic engineering is a powerful tool for the production of valuable chemicals (Jones et al. 2015; Nielsen and Keasling 2016). Metabolic engineering mainly includes static metabolic engineering and dynamic metabolic engineering. Static metabolic engineering has been tried and proved to be effective for some targets (Holtz and Keasling 2010; Liu et al. 2015). Its main strategies include engineering promoter (Jin et al. 2019), ribosome binding site (Nowroozi et al. 2014; Salis et al. 2009), and gene copy number (Jones et al. 2000). However, when the intracellular metabolic flow is rewired, it will impair microbial growth and production (Hartline et al. 2021). Dynamic metabolic engineering can regulate gene expression according to the changes of intracellular state and environmental conditions, thereby alleviate the growth

✉ Feng Shi
shifeng@jiangnan.edu.cn

1 State Key Laboratory of Food Science and Technology, Jiangnan University, 1800 Lihu Avenue, Wuxi 214122, China

2 Key Laboratory of Industrial Biotechnology, Ministry of Education, School of Biotechnology, Jiangnan University, Wuxi 214122, China

3 International Joint Laboratory On Food Safety, Jiangnan University, Wuxi 214122, China

4 National Engineering Research Center of Cereal Fermentation and Food Biomanufacturing, Jiangnan University, Wuxi 214122, China

retardation and metabolic flow imbalance caused by static engineering, and significantly increase the yield of target products (Anesiadis et al. 2008; Liu et al. 2015). Dynamic control strategies mainly include optogenetics switch (Renicke and Taxis 2016), temperature sensing switch (Zhou et al. 2018), biomolecular-sensor devices (Yang et al. 2018; Zhang et al. 2012), RNA-based dynamic controller (Zhou et al. 2019), quorum sensing devices, and so on (Liu et al. 2021), which have been applied in many fields. Among them, biomolecular-sensor devices can sense the concentration of certain metabolites and thereby regulate gene expression mainly through transcription factor (TF)-promoter pairs. RNA-based dynamic controller such as riboswitch can sense the concentration of specific metabolites and thereby mediate the structural changes of RNA and regulate the expression of their downstream genes. For example, Farmer et al. constructed a dynamic control switch to regulate lycopene synthesis by using acetyl phosphate responsive TF-promoter (Farmer and Liao 2000). Zhou and Zeng used L-lysine (Lys)-responsive riboswitch to regulate Lys synthesis (Zhou and Zeng 2015).

Corynebacterium glutamicum is a gram-positive bacterium widely used in amino acid industry (Becker et al. 2018). Products produced by *C. glutamicum* are generally recognized as safe. However, unlike *Escherichia coli* and *Saccharomyces cerevisiae*, there are only a few dynamic regulatory elements that have been well characterized and applied for metabolic engineering in *C. glutamicum* (Venayak et al. 2015). These tools mainly include the Lrp-P_{brnFE} biosensor that can upregulate gene expression by sensing branched chain amino acids (BCAAs) and L-methionine (Met) (Mustafi et al. 2012; Tan et al. 2020), the P_{ilvBNC} attenuator that can downregulate gene expression by responding to BCAAs (Morbach et al. 2000), the LysG-P_{lysE} biosensor upregulating gene expression by sensing Lys, L-histidine, and L-arginine (Kortmann et al. 2019), the Lys riboswitch that can turn off gene expression by binding Lys (Zhou and Zeng 2015), and the ShiR-P_{shiA} biosensor responding to shikimic acid (Liu et al. 2018).

The TF-based biosensor Lrp-P_{brnFE} has been used to dynamically regulate *odhI* expression and α-ketoglutarate (α-KG) supply for 4-hydroxyisoleucine (4-HIL) biosynthesis in *C. glutamicum* (Zhang et al. 2018). Quite recently, this biosensor has been further mutated and the modified strong biosensor Lrp-P_{brnFE}N was used to positively regulate the expression of *odhI* and *vgb*, resulting in a significant increase in the yield of 4-HIL (Tan et al. 2020). Besides the TF-based biosensor, attenuator and riboswitch were also used to regulate gene expression by sensing metabolite concentration. The P_{ilvBNC} promoter region of *C. glutamicum* contains an attenuator, which can also sense the concentration of BCAAs (Morbach et al. 2000). P_{ilvBNC} was used to attenuate and regulate *icd* expression, which increased the production of L-leucine (Leu) (Luo et al. 2021). P_{ilvBNC} was also used to attenuate and regulate the expression of *odhA* gene, which increased the production of 4-HIL (Zhang et al. 2018). The *odhA* gene encodes the E1 subunit of α-ketoglutarate dehydrogenase complex (ODHC). Riboswitch is a regulatory fragment located in the 5′ untranslated region (UTR) of mRNA. Riboswitch can detect and bind small molecule metabolites and then mediate the change of the RNA secondary structure, thereby affecting transcription termination and/or translation initiation (Winkler and Breaker 2005). Lys riboswitch has been successfully applied to Lys production. Zhou and Zeng used Lys-OFF riboswitch from *E. coli* to regulate *gltA* expression in *C. glutamicum*, which increased Lys production (Zhou and Zeng 2015). However, the Lys riboswitch has never been reported to be used in the synthesis of 4-HIL in *C. glutamicum*.

4-HIL can promote insulin secretion and decrease insulin resistance; thus, it is a promising drug for diabetes (Yang et al. 2020; Zafar and Gao 2016). Isoleucine dioxygenase (IDO) can catalyze the hydroxylation of C-4 of L-isoleucine (Ile) to form 4-HIL by consuming O_2, and α-KG is oxidized to succinic acid at the same time (Smirnov et al. 2010). In our previous study, the *ido* gene was expressed in an Ile producing strain *C. glutamicum* SN01 for de novo biosynthesis of 4-HIL (Shi et al. 2015). Subsequently, the yield of 4-HIL was further improved by static metabolic engineering (Shi et al. 2016, 2018, 2019, 2020). However, due to the inhibition of IDO by the excess substrate Ile and the requirement of coordinated supply of three substrates, it is difficult to increase the yield of 4-HIL by using the common static metabolic strategies. Then, the Lrp-P_{brnFE}N biosensor was used to dynamically upregulate IDO activity and the supply of α-KG and oxygen according to Ile concentration. The 4-HIL production was increased to 135.3 mM (Tan et al. 2020). However, during fermenting in a bioreactor, Ile accumulated too fast, which exacerbated the substrate inhibition and made the yield of 4-HIL unable to increase further. Meanwhile, a large amount of Lys was produced. Therefore, in addition to the upregulation of the downstream pathway for converting Ile to 4-HIL, it is necessary to dynamically regulate the upstream pathway for synthesizing Ile to avoid substrate inhibition. Meanwhile the synthesis pathway of by-product Lys shall be dynamically downregulated.

In this study, a triple-functional dynamic control system was designed to regulate the synthesis of 4-HIL. In order to accelerate the conversion of Ile to 4-HIL, the codon-optimized *ido* was regulated by the Lrp-P_{brnFE}N biosensor. This Ile biosensor was then used to dynamically upregulate the supply of other two substrates α-KG and oxygen. Meanwhile, in order to balance the supply of Ile and promote the conversion of Ile to 4-HIL, Ile attenuator P_{ilvBNC} was used to dynamically downregulate the expression of *ilvA*, a key gene in Ile synthesis pathway. Finally, in order to reduce the concentration of by-product Lys, the Lys-OFF riboswitch from *E. coli* MG1655 was used to negatively regulate the

expression of *dapA*, the key gene in Lys synthesis pathway (Fig. 1). The excellent strains with high yield of 4-HIL and no by-products or extremely low by-products content were obtained.

Materials and methods

Bacterial strains, plasmids, and culture conditions

The bacterial strains and plasmids used in this study are listed in Table 1. *E. coli* JM109 was used for plasmid construction and propagation. *E. coli* was cultivated at 37 °C and 200 rpm in Luria–Bertani (LB) medium. *C. glutamicum* ssp. *lactofermentum* SN01, an Ile-producing strain, was used for expressing target genes and synthesizing 4-HIL. SN01 was deposited into the China Center for Type Culture Collection (CCTCC) with accession number CCTCC M 2,014,410. The *C. glutamicum* strain was cultivated at 30 °C and 200 rpm in LBB medium (5 g/L tryptone, 2.5 g/L yeast extract, 5 g/L NaCl, and 18.5 g/L brain heart infusion powder). When necessary, 30 mg/L kanamycin or 10 mg/L chloramphenicol was added to the media.

Construction of dynamic modulation plasmids and strains

All primers used in this study are listed in Table 2. According to previous studies on Ile biosensors, seven inductive promoters of $P_{brnFE}N$ which can be induced by Ile, i.e., the native P_{brnFE} (designated as $P_{brnFE}0$) and the modified $P_{brnFE}1$, $P_{brnFE}5$, $P_{brnFE}D5$, $P_{brnFE}7$, $P_{brnFE}9$, and $P_{brnFE}13$, were designed for expressing target genes (Tan et al. 2020). $P_{brnFE}D5$ contains two promoter regions, which correspond to $P_{brnFE}5$ and the natural $P_{brnFE}0$ promoter, respectively. Firstly, the parent plasmid pIL-I^U was constructed to dynamically control *ido* expression. Before construction, the codon-optimized *ido* gene (*ido*^{U}) was synthesized. Its sequence was submitted to the GenBank with accession number OM541951. *ido*^{U} was ligated into pJYW-4 vector (Hu et al. 2014) to form the static expression plasmid pJYW-4-*ido*^{U}. It was transformed into *C. glutamicum* SN01,

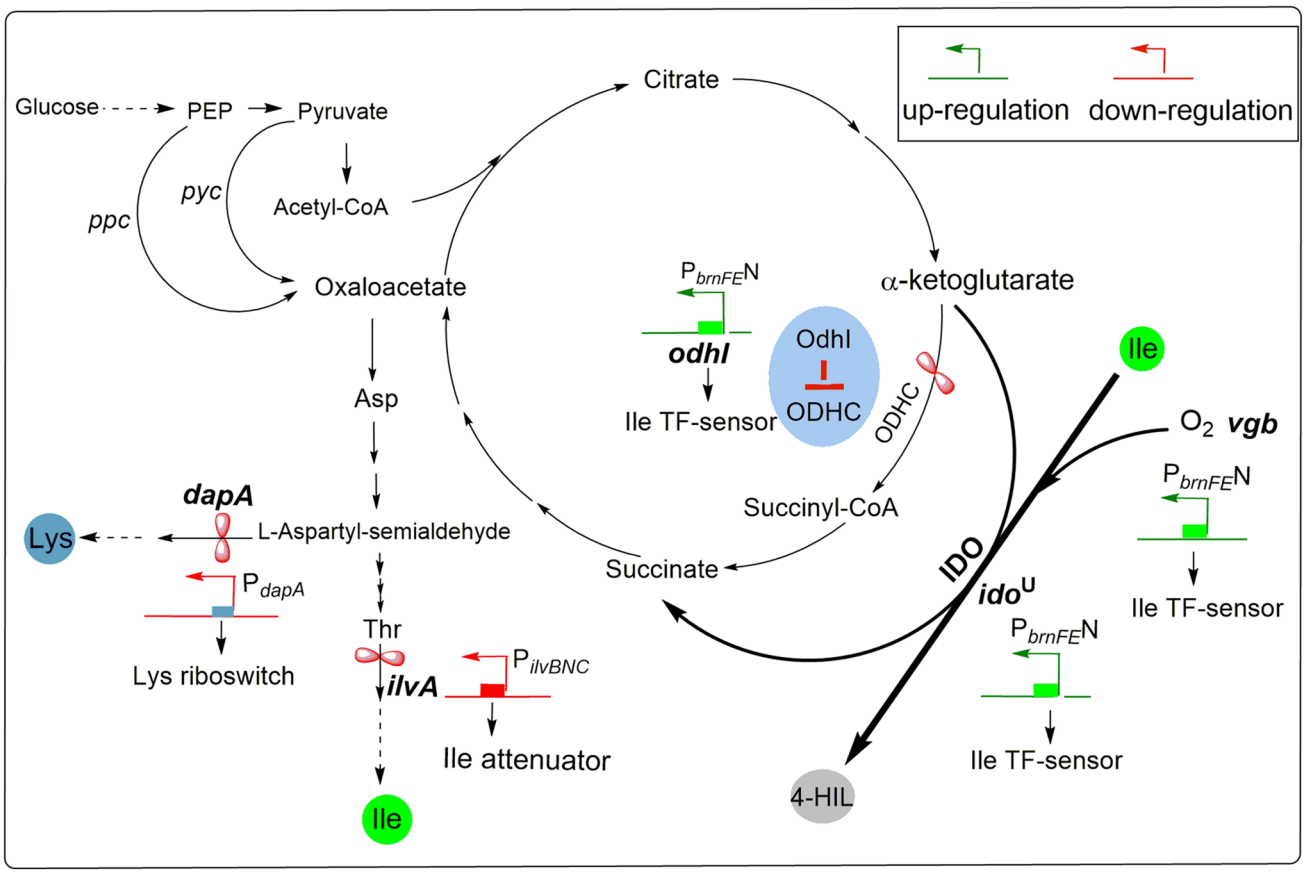

Fig. 1 The de novo biosynthetic pathway and metabolic engineering strategies of 4-HIL in recombinant *C. glutamicum* ssp. *lactofermentum* SN01. The dashed lines indicate the multi-step reaction. The heavy lines indicate the enhanced reaction. The red petals indicate the metabolic repression

Table 1 Bacterial strains and plasmids used in this study

Strains or plasmids	Characteristics	Source
JM109	*E. coli* gene-cloning strain	Novagen
SN01	Ile-producing strain of *C. glutamicum* ssp. *lactofermentum*	CCTCC
SI	SN01 harboring pJYW-4-*ido*^{U}	This work
D-RS	Integration of Lys-OFF riboswitch before *dapA* gene in SN01	This work
D-$_{N}$I	SN01 harboring pIL-$_{N}$I^{U}	This work
D-$_{N}$I$_{N}$O$_{N}$V	SN01 harboring pIL-$_{N}$I$^{U}{}_{N}$O$_{N}$V	This work
D-$_{N}$I$_{N}$O$_{N}$VPA	SN01 harboring pIL-$_{N}$I$^{U}{}_{N}$O$_{N}$VPA	This work
D-$_{N}$IPA	SN01 harboring pIL-$_{N}$I^{U}PA	This work
D-RS-$_{N}$IPA	D-RS harboring pIL-$_{N}$I^{U}PA	This work
D-RS-$_{N}$I$_{N}$O$_{N}$VPA	D-RS harboring pIL-$_{N}$I$^{U}{}_{N}$O$_{N}$VPA	This work
ATCC13032	Wild type *C. glutamicum*	ATCC
13,032-P$_{ilvBNC}$-*egfp*	*C. glutamicum* ATCC13032 harboring pJYW-4-P$_{ilvBNC}$-*egfp*	This work
pJYW-4	Constitutive expression vector of *C. glutamicum*, Km^{R}	Lab stock
pJYW-4-*ido*^{U}	pJYW-4 harboring the codon-optimized *ido* gene of *B. thuringiensis* YBT-1520 under P$_{tacM}$ promoter	This work
pK18mobsacB	Cloning vector of *E. coli*, Km^{R}	Lab stock
pK18-P$_{dapA}$-LysRS	pK18mobsacB derivative, P$_{dapA}$::P$_{dapA}$-Lys-OFF riboswitch replacing plasmid	This work
pIL-I	Derivative of pJYW-4 in which P$_{tacM}$ is replaced by *lrp* and P$_{brnFE}$-controlled *ido*	Lab stock
pIL-I^{U}	Derivative of pIL-I in which the codon of *ido* was optimized	This work
pIL-$_{N}$I^{U}	Derivative of pIL-I^{U} in which P$_{brnFE}$ is replaced by modified P$_{brnFE}$N	This work
pIL-$_{N}$I$^{U}{}_{N}$O$_{N}$V	Derivative of pIL-$_{N}$I^{U} that co-expresses P$_{brnFE}$N-controlled *odhI* and P$_{brnFE}$N-controlled *vgb*	This work
pIL-$_{N}$I^{U}PA	Derivative of pIL-$_{N}$I^{U} that co-expresses P$_{ilvBNC}$-controlled *ilvA*	This work
pIL-$_{N}$I$^{U}{}_{N}$O$_{N}$VPA	Derivative of pIL-$_{N}$I$^{U}{}_{N}$O$_{N}$V that co-expresses P$_{ilvBNC}$-controlled *ilvA*	This work
pJYW-4-*egfp*	pJYW-4 harboring the enhanced green fluorescence protein gene *egfp* under P$_{tacM}$ promoter	Lab stock
pJYW-4-P$_{ilvBNC}$-*egfp*	pJYW-4 harboring the *egfp* gene under P$_{ilvBNC}$ promoter	This work

generating the static strain SN01/pJYW-4-*ido*^{U}, renamed S-I. The *lrp*-P$_{brnFE}$N fragment and *ido*^{U} gene were amplified, fused, and ligated into the *Kpn*I- and *Bam*HI-digested pIL-I plasmid (Tan et al. 2020), generating seven dynamic plasmids pIL-$_{N}$I^{U}. These 7 plasmids were transformed into *C. glutamicum* SN01, generating 7 strains SN01/pIL-$_{N}$I^{U}, renamed D-$_{N}$I. Secondly, the plasmids pIL-$_{N}$I$^{U}{}_{N}$O$_{N}$V were constructed to dynamically modulate *ido*^{U}, *odhI*, and *vgb* expression. The 9 P$_{brnFE}$N-*odhI*-P$_{brnFE}$N-*vgb* fragments were amplified from plasmid pIL-$_{7}$I$_{N}$O$_{N}$V ($N=0, 1, 7$) (Tan et al. 2020) and then ligated into the 6 pIL-$_{N}$I^{U} ($N=0, 1, 5, D5, 7, 9$) vectors to form $6\times9=54$ pIL-$_{N}$I$^{U}{}_{N}$O$_{N}$V plasmids. These plasmids were transformed into *C. glutamicum* SN01, generating 54 strains SN01/pIL-$_{N}$I$^{U}{}_{N}$O$_{N}$V, renamed D-$_{N}$I$_{N}$O$_{N}$V. Thirdly, the plasmids pIL-$_{N}$I^{U}PA were constructed to positively regulate *ido*^{U} by Lrp-P$_{brnFE}$N and negatively regulate *ilvA* by P$_{ilvBNC}$. The fragments of P$_{ilvBNC}$ and *ilvA* were amplified from SN01, fused, and ligated into 6 pIL-$_{N}$I^{U} vectors to form 6 pIL-$_{N}$I^{U}PA plasmids. These 6 plasmids were transformed into *C. glutamicum* SN01, generating 6 strains SN01/pIL-$_{N}$I^{U}PA, renamed D-$_{N}$IPA. Fourthly, the plasmids pIL-$_{N}$I$^{U}{}_{N}$O$_{N}$VPA were constructed to positively regulate *ido*^{U}, *odhI*, and *vgb* by Lrp-P$_{brnFE}$N and negatively regulate *ilvA* by P$_{ilvBNC}$. The fragment of P$_{ilvBNC}$-*ilvA* was amplified and ligated into 12 pIL-$_{N}$I$^{U}{}_{N}$O$_{N}$V vectors to form 12 pIL-$_{N}$I$^{U}{}_{N}$O$_{N}$VPA plasmids. However, the pIL-$_{9}$I$^{U}{}_{7}$O$_{7}$V, pIL-$_{0}$I$^{U}{}_{7}$O$_{7}$V, and pIL-$_{D5}$I$^{U}{}_{7}$O$_{7}$V plasmids were failed to be constructed. These 9 plasmids were transformed into *C. glutamicum* SN01, generating 9 strains SN01/pIL-$_{N}$I$^{U}{}_{N}$O$_{N}$VPA, renamed D-$_{N}$I$_{N}$O$_{N}$VPA.

At last, the fluorescent reporter plasmid pJYW-4-P$_{ilvBNC}$-*egfp* was constructed. The fragments of P$_{ilvBNC}$ and *egfp* were amplified from SN01 and pJYW-4-*egfp*, respectively, fused, and ligated into pJYW-4 vector, resulting in the P$_{ilvBNC}$-regulated reporter plasmid pJYW-4-P$_{ilvBNC}$-*egfp*. This plasmid was then transformed into *C. glutamicum* ATCC 13,032, generating the strain 13,032-P$_{ilvBNC}$-*egfp*.

Integration of Lys-OFF riboswitch in the upstream of dapA gene in chromosome

The Lys-OFF riboswitch was introduced to dynamically control the expression of *dapA* gene and the synthesis of Lys. Based on pK18mobsacB editing system (Schäfer et al. 1994), the Lys-OFF riboswitch (Zhou and Zeng 2015) was integrated before the start codon of *dapA* gene in *C. glutamicum* ssp. *lactofermentum* SN01 and the synthesis of Lys was negative regulated by intracellular Lys

Table 2 Primes used in this study

Primers	Sequences (5′-3′)	Restriction sites	Description
Lrp-F(*Kpn*I)	ATTAGGTACC**TCA**CACCTGGGGGCGAGCTGGTTTC	*Kpn*I	For *lrp*-P_{brnFE}N amplification
P_{brnFE}N-R	GAGAAGCCGGACATCTT**CAT**CCTATAA*CTCCTTCT*CTC		
ido^{U}-F	**ATG**AAGATGTCCGGCTTCTC		For *ido*^{U} amplification
ido^{U}-R(*Bam*HI)	TATGGATCC**TTA**CTTGGTCTCCTTGTAGG	*Bam*HI	
P_{brnFE}N-odhI-F	ACAAGGAGACCAAG**TAA**ACGAATTCGCTAAGCTC		For P_{brnFE}N-*odhI*-P_{brnFE}N-*vgb* amplification
vgb-R	AGCTCGAATTCGTCGAC**TTA**TTCAACCGCTTGAGC		
ido^{U}-P_{ilvBNC}-F	AGGAGACCAAG**TAA**GGATCCCCAAGATTAGCGCTG AAAAG		For P_{ilvBNC} amplification
P_{ilvBNC}-R	ACACGTATGTTTCACT**CAT**GACTTTCTGGCTCCTTTAC		
ilvA-F	**ATG**AGTGAAACATACGTGTC		For *ilvA* amplification
ilvA-R(1)	AATTCGTCGACGGATCC**TTA**GGTCAAGTATTCGTAC		
vgb-P_{ilvBNC}-F	ACGCTCAAGCGGTTGAA**TAA**GTCGACCCAAGATTA GCGCTGA AA		For P_{ilvBNC}-*ilvA* amplification
ilvA-R(2)	TCTAGAGAGCTCGAATTC**TTA**GGTCAAGTATTCGTAC		
dapA-U-F	ATAGTCGACGTGGTGCCCACTCTCATC	*Sal*I	For *dapA*-Up amplification
dapA-U-R	GGTAGTACATAGAGTTCAAGGTTACCTTCTT		
dapA-D-F	ACAGAAGGAGTTATAGG**ATG**AGCACAGGTTTAAC		For *dapA*-Dn amplification
dapA-D-R	ATAGTCGACTTAGTGGGTCATCGCCTG	*Sal*I	
Lys-OFF-F	AGAAGGTAACCTTGAACTCTATGTACTACCTGCGCTAG		For Lys-OFF riboswitch amplification
Lys-OFF-R	CT**CAT**CCTATAACTCCTTCTGTGTCAGGGGATCCA TTTTC		
P_{ilvBNC}-*egfp*-F	AGCTGTTGACAATTAATCATCGTGTCCAAGATTAGC GCTGAAAAG		For P_{ilvBNC} amplification
P_{ilvBNC}-*egfp*-R	GACTTTCTGGCTCCTTTACTAA		
egfp-F	AAAGGAGCCAGAAAGTC**ATG**GTTTCCAAGGGCGAG		For *egfp* amplification
egfp-R	ACAATTCCACACATGGTACC**TTA**CTTGTACAGCTC GTCC		

The start and stop codons are indicated in boldface. The restriction sites are underlined. The ribosomal binding sites are italicized

concentration. The upstream and downstream homologous arms of *dapA* were amplified from *C. glutamicum* SN01. The Lys-OFF riboswitch was amplified from *E. coli* MG1655. Then the fragments of *dapA*-U, Lys-OFF riboswitch, and *dapA*-D were linked by overlap PCR to obtain *dapA*-U-LysRS-*dapA*-D fragment. The *dapA*-U-LysRS-*dapA*-D fragment was ligated into the *Sal*I-digested pK18mobsacB vector, resulting in the integrating plasmid pK18mobsacB-P_{dapA}-LysRS. This plasmid was transformed into *C. glutamicum* ssp. *lactofermentum* SN01 for two rounds of homologous recombination to get the recombinant strain SN01 P_{dapA}::P_{dapA}-LysRS (designated as D-RS). Finally, the above 6 dynamic regulatory plasmids of pIL-$_{N}$I^{U}PA were transformed into D-RS, resulting in 6 strains D-RS-$_{N}$IPA. Meanwhile, the above dynamic regulatory plasmids of pIL-$_{7}$I$^{U}{}_{7}$O$_{1}$VPA with high yield of 4-HIL were transformed into D-RS for expression and resulted in strain D-RS-$_{7}$I$_{7}$O$_{1}$VPA.

4-HIL fermentation

4-HIL fermentation of statically and dynamically controlled *C. glutamicum* ssp. *lactofermentum* strains in shake flasks were conducted as described previously, using optimized fermentation medium (Shi et al. 2019). The cell density, residual glucose, pH, and amino acid and 4-HIL concentrations in the fermentation broth were measured every 24 h by the methods described previously (Shi et al. 2018). The residual glucose concentration was measured by an SBA-40C biosensor (Institute of Biology, Shandong Academy of Science, China). The pH was measured by a pH electrode (Mettler-Toledo, Germany). The amino acids and 4-HIL concentrations were detected by high performance liquid chromatography (HPLC) analysis (Shi et al. 2016). Firstly, protein impurities in the fermentation broth were precipitated with 5% trichloroacetic acid, and then, the precipitate was removed by centrifugation and the supernatant

was diluted 20 times for HPLC analysis. The amino acids and 4-HIL concentrations were determined by Agilent 1200 HPLC detector equipped with a Thermo ODS-2 HYPERSIL C18 column (250 mm × 4.6 mm, USA) using the *ortho*-phthalaldehyde precolumn derivatization method. The conversion ratio of Ile to 4-HIL was calculated as the moles of 4-HIL divided by the total moles of Ile and 4-HIL. To determine the intracellular amino acids' concentrations, the cell sedimentation was collected by centrifugation, then washed, and disrupted as described previously to isolate the intracellular amino acids (Shi et al. 2016). The intracellular concentration was calculated with the intracellular volume of 1.6 mL/g dry cell weight (DCW). The DCW (g/L) was calculated according to an experimentally determined formula: $DCW = 0.6495 \times OD_{562} - 2.7925$.

Fluorescence assays

The fluorescent reporter strain 13,032-P_{ilvBNC}-*egfp* was precultured in LBB medium for 12 h, and the cells were washed and resuspended with 0.9% NaCl solution. Then, the cell resuspension was transferred to the Ile restricted medium (25 g/L glucose·H_2O, 1 g/L KH_2PO_4, 0.5 g/L $(NH_4)_2SO_2$, 0.75 g/L $MgSO_4$, 1.0 g/L $FeSO_4$, 10 μg/L biotin, 1 mg/L thiamine, and 0–10 mM Ile, pH 7.20) with the initial OD_{562} of 0.05 and cultured for 24 h. At every 4 h, the cultured cells were collected, washed with, and resuspended in 0.9% NaCl solution. Subsequently, the cell suspension was transferred to a black 96-well plate with a transparent bottom. Green fluorescence was detected by the Cytation5 (BiotTek) with an excitation filter of 479/20 nm and an emission filter of 520/20 nm.

Results

Positive regulation of codon-optimized ido expression by Ile biosensor

Isoleucine dioxygenase (coded by *ido*) that catalyzes the conversion of Ile to 4-HIL is a key enzyme for de novo synthesis of 4-HIL. The expression level of *ido* and the enzyme activity of IDO are very important for the synthesis of 4-HIL. In the previous research, the strong promoter P_{tacM} was used to constitutively express *ido* in plasmid pJYW-4-*ido* of strain SN02 as well as in other plasmids such as pJYW-4-*imi3*-*vgb* of strain SZ05 (Shi et al. 2015, 2019). However, constitutive expression brought metabolic burden to cells, and intracellular resources would be continuously utilized to synthesize IDO. Then Ile biosensor Lrp-P_{brnFE}N was used to dynamically control the expression of *ido*, because Ile is the direct precursor of 4-HIL synthesis. P_{brnFE}N were several modified promoters of native P_{brnFE} promoter with different strengths. They were obtained from the *lrp*-P_{brnFE} mutant library through *tetA* dual genetic selection, and their − 10 region and spacer between − 35 and − 10 regions were modified (Tan et al. 2020). Although the 4-HIL titer was comparable to that of P_{tacM}-controlled *ido* expressing strain SN02, the titer was not ideal. Besides the Ile sensitivity and threshold of Lrp-P_{brnFE}N biosensors as well as their strength after activation, the preference of *ido* codons and burden expression of other proteins may also influence the synthesis of 4-HIL. So, the codon-optimized *ido* gene was expressed and dynamically controlled here by several Ile biosensors Lrp-P_{brnFE}N (Fig. 2A). The resulting seven plasmids pIL-$_N$I^U were transferred into SN01 to obtain D-$_N$I strains (N = 0, 1, 5, D5, 7, 9, 13). And the pJYW-4-*ido*^{U} plasmid was transferred into SN01 strain to obtain SI as static control strain.

During the whole fermentation process, D-$_7$I grew slightly faster, while other 6 D-$_N$I strains showed similar growth rate to SI. However, the sugar consumption of 7 D-$_N$I strains were similar to each other and were slightly faster than SI (Fig. 2B). Although the 4-HIL titer of D-$_{13}$I was extremely low, the overall 4-HIL titer of other 6 D-$_N$I strains was high and similar (Fig. 2C). And compared with the *ido* expression strains ST01–ST06 controlled by the same biosensor (Tan et al. 2020), the 4-HIL production of *ido*^{U}-expressing strains D-$_N$I improved overall. Finally, D-$_1$I, D-$_0$I, D-$_{D5}$I, and D-$_5$I accumulated 111.1 ± 0.8, 106.3 ± 7.1, 97.5 ± 5.7 and 92.0 ± 6.7 mM 4-HIL, respectively, which was 23.5%, 18.2%, 8.4%, and 2.3% higher than SI (89.9 ± 2.5 mM) and 57.8%, 51.0%, 38.4%, and 30.7% higher than the best *ido*-expressing strain ST04 (70.4 ± 8.2 mM) controlled by the same biosensors. While D-$_7$I and D-$_9$I accumulated 84.2 ± 0.7 and 79.5 ± 2.8 mM 4-HIL respectively, which was 6.4% and 11.6% lower than SI and 19.6% and 12.9% higher than the best *ido*-expressing strain ST04 controlled by the same biosensors. The above results suggested that the expression of codon-optimized *ido*^{U} gene increased the IDO activity, which enhanced the conversion of Ile to 4-HIL. Dynamically regulating the expression of *ido*^{U} by Lrp-P_{brnFE}N biosensors was more conducive to the synthesis of 4-HIL than dynamically regulating the expression of *ido* by the same biosensors.

In D-$_1$I, Ile accumulated rapidly in 24 h and then reduced gradually to 0 mM during 24–96 h, while in D-$_{D5}$I and D-$_7$I, Ile was consumed before 48 h (Fig. 2D). The synthesis of 4-HIL may be limited in these three strains due to the insufficient supply of Ile. In D-$_0$I, D-$_5$I, and D-$_9$I, Ile accumulated continuously in 72 h and slightly decreased and fluctuated thereafter (Fig. 2D). Finally, 40–80 mM of Ile was remained and not converted to 4-HIL. Besides the substrate Ile, the α-KG and oxygen are also required in the synthesis of 4-HIL. The 4-HIL titer of these three strains did not increase after 96 h, likely due to the insufficient supply

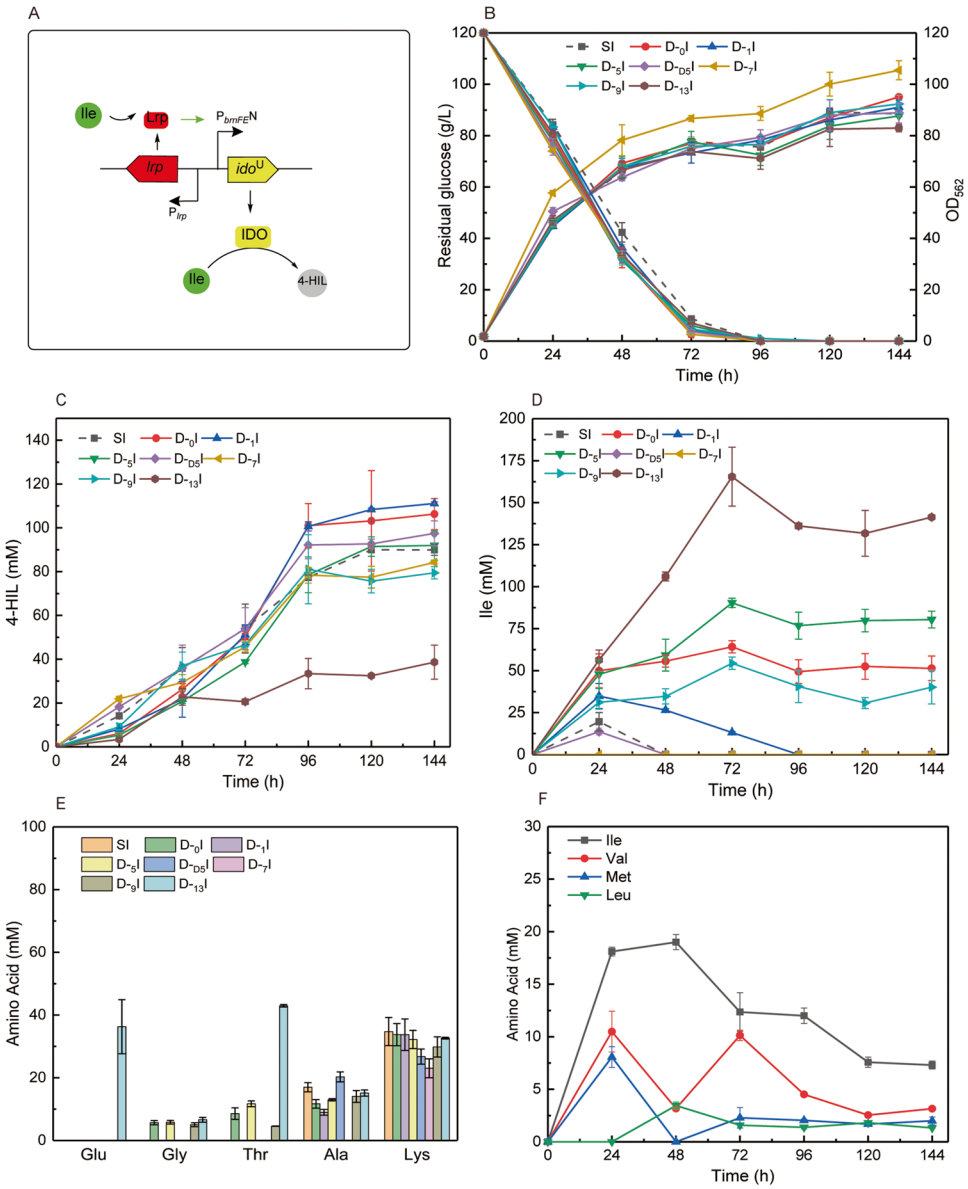

Fig. 2 Regulation mode and 4-HIL fermentation of strains $D\text{-}_NI$. **A** Diagram of the Lrp-$P_{brnFE}N$ regulation circuit. Transcription factor Lrp combines with BCAAs. Then Ile-Lrp complex binds to $P_{brnFE}N$, thereby activates the transcription of $P_{brnFE}N$-controlled ido^U gene, and promotes the conversion of Ile to 4-HIL according to Ile concentration. **B** Cell growth and glucose consumption. **C** 4-HIL accumulation. **D** Ile accumulation. **E** Other amino acids concentration at 144 h. **F** Intracellular accumulation of Ile, Val, Met and Leu in $D\text{-}_1I$

of α-KG and oxygen. However, in the $D\text{-}_{13}I$ strain, the yield of 4-HIL was relatively low, and a large amount of Ile was not converted into 4-HIL (Fig. 2C and 2D). This result suggested that the strength of $P_{brnFE}13$ was low, which led to the low activity of IDO enzyme, thus triggering the strong inhibition of IDO by excess Ile and the extra accumulation of by-product L-threonine (Thr), the precursor of Ile synthesis. Therefore, this strain was discarded in the subsequent study. In all of the 7 recombinant $D\text{-}_NI$ strains, the content of by-product Lys was high, while other by-products were almost absent or showed extremely low content (Fig. 2E). Thereby, besides the dynamic control of the *ido* expression, the supply of various substrates, such as oxygen, α-KG, and Ile, should be appropriately controlled.

Lrp responds to Ile and also to Met, L-valine (Val) and Leu. The intracellular or extracellular accumulation of Val, Met, and Leu may also affect the activated level of Lrp-$P_{brnFE}N$ biosensors and the yield of 4-HIL. Therefore, the intracellular and extracellular contents of Ile, Val, Met, and Leu in the best ido^U-expressing strain $D\text{-}_1I$ were determined. Its extracellular contents of Val, Met, and Leu were very low (data not shown), while its intracellular contents of Ile, Val, Met, and Leu were 19.0–7.3 mM, 10.5–3.2 mM, 8.1–1.7 mM, and 3.4–1.3 mM, respectively (Fig. 2F). Meanwhile, these intracellular contents were relatively high during 24–96 h, but much low thereafter, in accordance with the quick accumulation of 4-HIL during 24–96 h and slow thereafter (Fig. 2C).

In the previous study, P_{brnFE}N promoters were divided into strong (P_{brnFE}7), medium (P_{brnFE}1, P_{brnFE}5) and weak (P_{brnFE}0, P_{brnFE}9, P_{brnFE}13) groups, and the 4-HIL yield of the *ido*-expressing strain dynamically controlled by strong promoter P_{brnFE}7 was the highest (Tan et al. 2020). Here, the 4-HIL yield of the ido^U-expressing strain under P_{brnFE}7 promoter was also high. As expected, the 4-HIL yield of ido^U-expressing strains controlled by other P_{brnFE}N promoters has been improved in greater degrees, which indicated that the IDO activity of codon-optimized ido^U-expressing strains is improved, and all the P_{brnFE}0, P_{brnFE}1, P_{brnFE}5, P_{brnFE}D5, P_{brnFE}7, and P_{brnFE}9 were strong for expressing ido^U. Therefore, the strains D-$_N$I (N = 0, 1, 5, D5, 7, or 9) with high yield of 4-HIL were used for further study.

Positive regulation of ido.^{U}, odhI, and vgb expression by Ile biosensor

Although the synthesis of 4-HIL was improved in the above six D-$_N$I strains, Ile was used up too early in D-$_{D5}$I and D-$_7$I, while in D-$_0$I, D-$_5$I, and D-$_9$I, Ile was no longer converted to 4-HIL in the later fermentation stage. The substrates required for the synthesis of 4-HIL include not only Ile, but also α-KG and O_2. Therefore, *odhI* and *vgb* were overexpressed in this section to promote the coordinated supply of the other two substrates, α-KG and O_2. The unphosphorylated OdhI can bind to OdhA subunit of ODHC, thus inhibiting ODHC activity and finally intercepting more α-KG for the synthesis of 4-HIL. The *vgb* gene encodes *Vitreoscilla* hemoglobin VHb, which can increase the uptake of O_2 by cells. However, excessive O_2 intake will form free radicals and cause damage to cells. In our previous studies, P_{brnFE}7 with high strength, P_{brnFE}1 with medium strength and P_{brnFE}0 with low strength were used to control *odhI* and *vgb* expression in dynamic *ido*-expression strains, which promoted the titer of 4-HIL to 135.34 mM (Tan et al. 2020). Therefore, in this section, these 3 P_{brnFE}N promoters were used to positively regulate *odhI* and *vgb* expression on the basis of 6 dynamic ido^U-expression plasmids pIL-$_N$I^U (Fig. 3A). The obtained 54 plasmids of pIL-$_N$I^U_NO$_N$V were transformed into SN01, and 54 tri-gene dynamic regulatory strains named D-$_N$I$_N$O$_N$V were obtained.

In the 9 D-$_0$I$_N$O$_N$V strains, D-$_0$I$_0$O$_1$V, D-$_0$I$_1$O$_1$V, D-$_0$I$_1$O$_7$V, and D-$_0$I$_7$O$_7$V accumulated 119.4 ± 22.4, 125.3 ± 27.6, 134.5 ± 12.3, and 141.1 ± 15.5 mM 4-HIL, respectively (Fig. 3B), which increased by 12.3%, 17.9%, 26.5%, and 32.7% compared with D-$_0$I (106.3 ± 7.1 mM). While the 4-HIL yield of D-$_0$I$_0$O$_7$V (92.1 ± 18.8 mM) was a little lower than that of D-$_0$I, but it was still 2.4% higher than that of SI (89.9 ± 2.5 mM). In the 9 D-$_9$I$_N$O$_N$V strains, D-$_9$I$_0$O$_0$V, D-$_9$I$_0$O$_1$V, D-$_9$I$_0$O$_7$V, and D-$_9$I$_7$O$_7$V accumulated 107.3 ± 17.9, 115.5 ± 21.1, 103.2 ± 4.2, and 131.2 ± 4.5 mM 4-HIL, respectively (Fig. 3B), which increased by 35.0%, 45.4%, 29.8%, and 65.1% compared with D-$_9$I (79.5 ± 2.8 mM). The above results indicated that the dynamic supply of α-KG and oxygen could promote the remaining Ile in D-$_0$I and D-$_9$I to convert into 4-HIL and thereby further increase the yield of 4-HIL. In the 9 D-$_1$I$_N$O$_N$V strains, only D-$_1$I$_0$O$_7$V could produce more 4-HIL (Fig. 3B), but its yield of 4-HIL was lower than those of D-$_1$I and SI, so the D-$_1$I$_0$O$_7$V strain was discarded in the subsequent studies. Perhaps the supply of three substrates in D-$_1$I is relatively coordinated with the synthesis of 4-HIL, making further supply of α-KG and oxygen ineffective in D-$_1$I. In the 9 D-$_5$I$_N$O$_N$V strains, 9 D-$_{D5}$I$_N$O$_N$V strains and 9 D-$_7$I$_N$O$_N$V strains, the 4-HIL yield of D-$_5$I$_0$O$_1$V (89.9 ± 10.8 mM) and D-$_{D5}$I$_7$O$_7$V (93.5 ± 12.2 mM) was similar to that of SI, and the 4-HIL yield of D-$_7$I$_7$O$_1$V (132.7 ± 13.3 mM) increased by 57.6% compared with D-$_7$I (84.20 ± 0.7 mM), while the 4-HIL yield of other strains were lower than that of D-$_5$I, D-$_{D5}$I, D-$_7$I, and SI (Fig. 3B). The scarcely improved 4-HIL production in these strains suggests that other reason such as the insufficient supply of Ile might also be a crucial constraint for 4-HIL synthesis. Thereby, dynamic regulation of Ile synthesis was performed in the next section. In addition, 12 strains of this section, i.e., D-$_5$I$_0$O$_1$V, D-$_{D5}$I$_7$O$_7$V, D-$_7$I$_7$O$_1$V, D-$_0$I$_0$O$_1$V, D-$_0$I$_1$O$_1$V, D-$_0$I$_7$O$_7$V, D-$_0$I$_0$O$_7$V, D-$_0$I$_1$O$_7$V, D-$_9$I$_0$O$_0$V, D-$_9$I$_0$O$_1$V, D-$_9$I$_0$O$_7$V, and D-$_9$I$_7$O$_7$V with higher 4-HIL yield than SI (89.9 ± 2.5 mM) were selected for further study.

To check the influence of Val, Met, and Leu on Ile biosensor and 4-HIL production, the intracellular and extracellular contents of Ile, Val, Met, and Leu as well as the effect of Val, Met, and Leu addition on 4-HIL fermentation were analyzed in the best tri-gene dynamic strain D-$_0$I$_7$O$_7$V. As shown in Fig. 3C, its intracellular contents of Val, Met, and Leu were a little high at 24 h and then fluctuated around 1–4 mM thereafter, while its extracellular contents could not be detected. These contents were much lower than that of Ile, indicating that the cellular response of Lrp-P_{brnFE}N biosensors to Val, Met, and Leu might be much lower than that to Ile. When separately adding 10 mM Val, 10 mM Met, or 10 mM Leu, cells grew a little slowly, and 4-HIL titers decreased to 69.5 ± 9.0, 96.0 ± 7.1, and 85.4 ± 0.7 mM, respectively (Fig. 3D), 50.7%, 32.0%, and 39.5% lower than that produced without addition. Thereby, the addition of Val, Met, and Leu could not promote 4-HIL production.

Bidirectional regulation of Ile synthesis and conversion

Ile is the direct precursor of 4-HIL, which is very important for the synthesis of 4-HIL. Therefore, in this section, the key gene for Ile synthesis, i.e., *ilvA* was expressed to strengthen the Ile supply. However, the activity of IDO is greatly inhibited by excessive Ile (Shi et al. 2016; Tan et al. 2020), so the

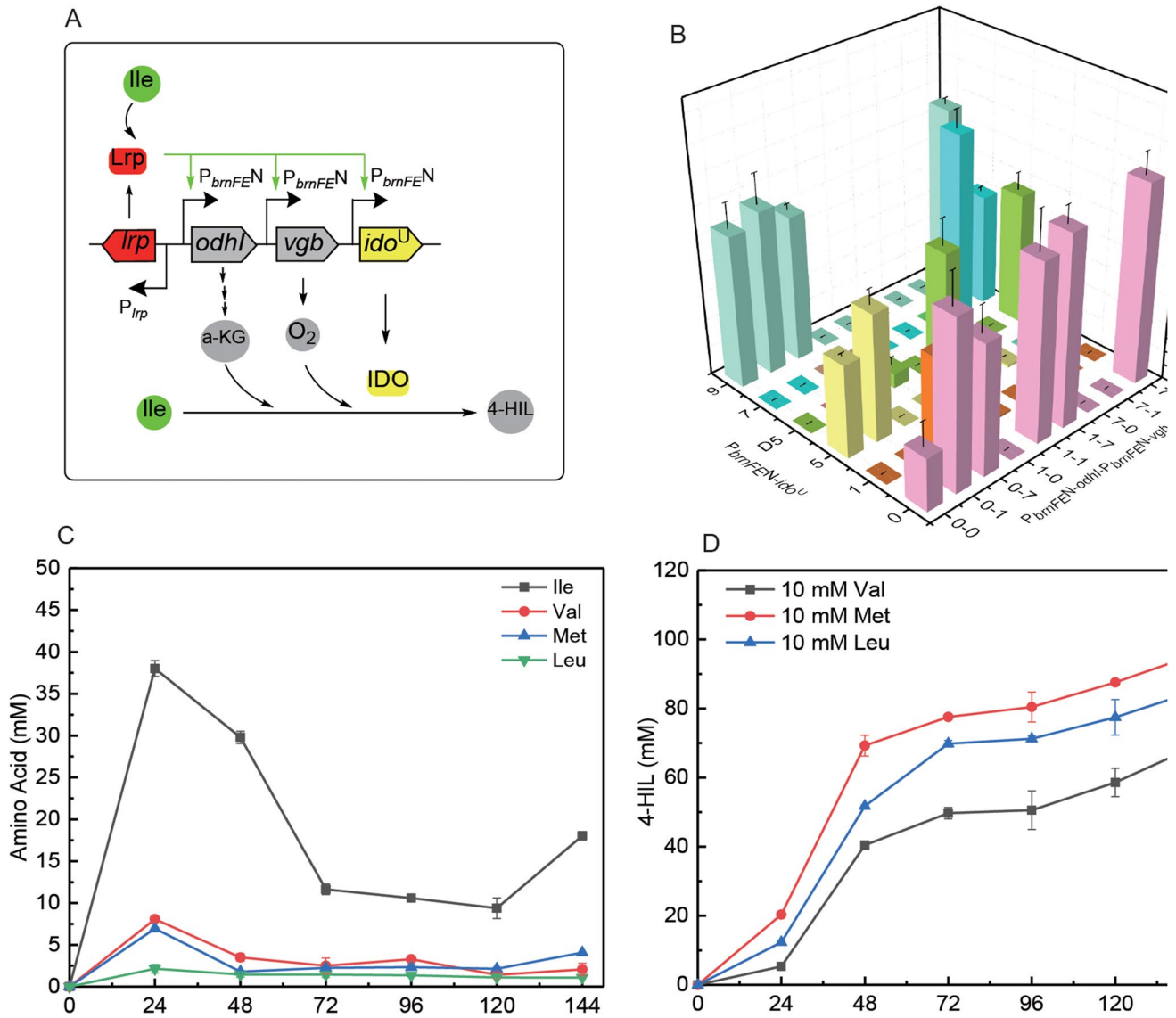

Fig. 3 Regulation circuit and 4-HIL production of strains D-$_{N}$I$_{N}$O$_{N}$V. **A** Diagram of regulation circuit. Lrp-P$_{brnFE}$N positively regulated the expression of *ido*^{U}, *odhI*, and *vgb* in response to intracellular Ile concentration. **B** 4-HIL production of D-$_{N}$I$_{N}$O$_{N}$V. **C** Intracellular accumulation of Ile, Val, Met, and Leu in D-$_{0}$I$_{7}$O$_{7}$V. **D** 4-HIL production of D-$_{0}$I$_{7}$O$_{7}$V after adding 10 mM Val, Met, or Leu

synthesis of Ile and the conversion of Ile to 4-HIL shall be carefully balanced. Thereby, the expression of *ilvA* was negatively regulated here by an Ile attenuator P$_{ilvBNC}$ on the basis of positive regulation of *idoU* by *lrp*-P$_{brnFE}$N in plasmids pIL-$_{N}$I^{U} (Fig. 4A), in order to balance the upstream supply and downstream conversion of Ile. Therefore, P$_{ilvBNC}$-*ilvA* was expressed in pIL-$_{N}$I^{U}, and six pIL-$_{N}$I^{U}PA plasmids were obtained. These plasmids were transformed into SN01 to obtain 6 strains with bidirectional dynamic regulations of 4-HIL synthesis, named D-$_{N}$IPA.

In the whole fermentation process, D-$_{1}$IPA and D-$_{5}$IPA grew slightly faster than their original strains D-$_{1}$I and D-$_{5}$I, while the other D-$_{N}$IPA strains grew slower than their original strains D-$_{N}$I. Correspondingly, D-$_{1}$IPA and D-$_{5}$IPA consumed sugar similarly to D-$_{1}$I and D-$_{5}$I, while other D-$_{N}$IPA strains consumed sugar slightly slower than their initial strains D-$_{N}$I (Fig. 4B). Eventually, 4-HIL titer of D-$_{D5}$IPA and D-$_{7}$IPA is 118.2 ± 14.2 mM and 123.2 ± 20.5 mM, respectively, which increased by 21.3% and 46.3% compared with D-$_{D5}$I and D-$_{7}$I. However, Ile accumulated rapidly to the highest value of about 40 mM before 48 h, declined rapidly to around 10 and 40 mM at 48–96 h, and fluctuated thereafter in D-$_{D5}$IPA and D-$_{7}$IPA (Fig. 4C, D). These results suggested that Ile was stably and continuously supplied in these two strains, which led to the continuous synthesis of 4-HIL. 4-HIL

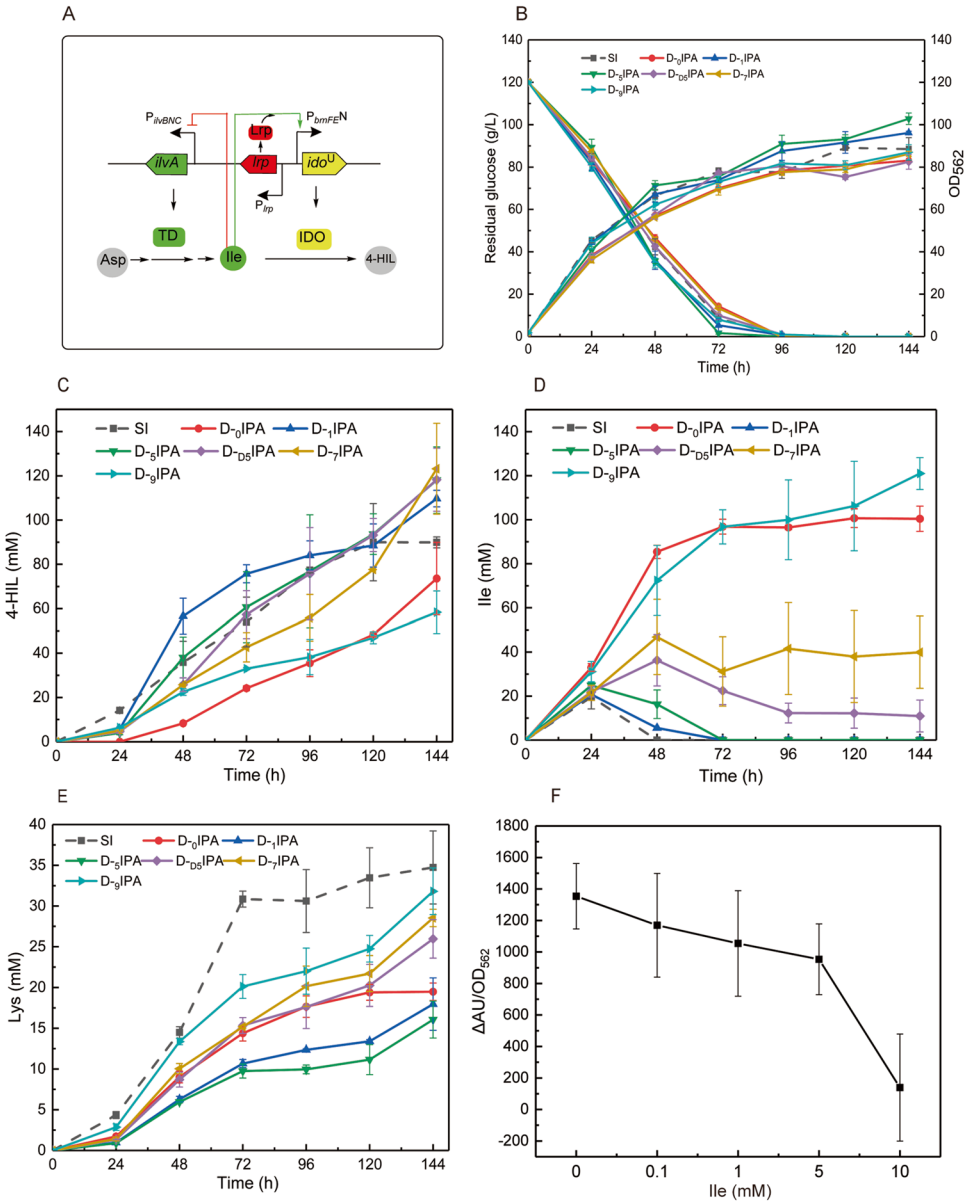

Fig. 4 Bidirectional regulating circuit and 4-HIL fermentation of strains D-$_N$IPA. **A** Diagram of the bidirectional regulation circuit. When the concentration of Ile is high, the expression of *ido*.^{U} is strengthened to enhance the downstream pathway of Ile conversion; meanwhile, the expression of *ilvA* is weakened to reduce the upstream pathway of Ile synthesis and thereby avoids substrate inhibition by excess Ile. When the concentration of Ile is low, the expression of *ilvA* is strengthened to enhance the Ile synthesis, thereby providing sufficient Ile for IDO reaction and 4-HIL synthesis. **B** Cell growth and glucose consumption. **C** 4-HIL accumulation. **D** Ile accumulation. **E** The by-product Lys accumulation. **F** Relative fluorescence intensity of 13,032-P$_{ilvBNC}$-*egfp* after adding 0.1–10 mM Ile

yields of D-$_1$IPA and D-$_5$IPA were 109.7 ± 3.7 mM and 118.0 ± 15.0 mM, respectively, which was similar to those of D-$_1$I and D-$_5$I. Meanwhile, the Ile concentration of these two strains increased to around 20 mM at 24 h and decreased to 0 mM at 72 h, but the 4-HIL concentration increased continuously in the middle stage of fermentation (Fig. 4C, D), suggesting that Ile has been continuously synthesized and immediately converted into 4-HIL in these two strains. Therefore, the metabolism between the upstream synthesis pathway and the downstream conversion pathway of Ile is relatively coordinated among the above four strains. However, D-$_0$IPA and D-$_9$IPA accumulated 73.6 ± 16.3 mM and 58.4 ± 9.6 mM 4-HIL, respectively, which decreased by 30.8% and 26.5% compared with D-$_0$I and D-$_9$I. Although their total sum of 4-HIL and Ile was relatively high, a large amount of Ile accumulated could not be converted and 4-HIL was slowly synthesized after 72 h (Fig. 4C, D). These results implied the insufficient supply of α-KG and/or O_2 and the excessive accumulation of Ile after P$_{ilvBNC}$-*ilvA* expression in these two strains. Although the growth of most D-$_N$IPA strains was slower, their synthesis of 4-HIL was improved compared with D-$_N$I in the first 72 h. The results indicated that the bidirectional dynamic regulation strategy alleviated the substrate inhibition and promoted the synthesis of 4-HIL. Therefore, the yield of 4-HIL of most strains increased, suggesting that the bidirectional dynamic regulation strategy had more advantages than the unidirectional dynamic adjustment strategy. However, D-$_N$IPA still accumulated a large amount of by-product Lys (Fig. 4E).

Since Ile secretion of some strains was still very high, the dose response of Ile attenuator P_{ilvBNC} was characterized with the fluorescence reporter eGFP. The reporter plasmid pJYW-4-P_{ilvBNC}-*egfp* was constructed and introduced into *C. glutamicum* ATCC13032 which hardly produced Ile. This reporter strain was cultured in the absence of Ile or presence of 0.1 mM, 1 mM, 5 mM, or 10 mM Ile. Although the growth of this strain in Ile-restricted medium was poor, the variation of its relative fluorescence intensity could be observed. The fluorescence decreased slightly in the presence of 0.1–5 mM Ile but significantly in the presence of 10 mM Ile (Fig. 4F). Therefore, the minimum Ile concentration which P_{ilvBNC} attenuator can respond to was 10 mM, and at that concentration, the P_{ilvBNC} would attenuate the expression of downstream genes.

Synergistically dynamic control of IDO activity and Ile, α-KG, O_2 supply

The above strains D-$_1$IPA, D-$_5$IPA, D-$_{D5}$IPA, and D-$_7$IPA possessed the improved 4-HIL synthesis through balancing the supply and hydroxylation of Ile. While in the second section, the 4-HIL production of 12 strains was improved significantly by upregulating the supply of O_2 and α-KG. Ile, α-KG, and O_2 are the three direct substrates of IDO reaction in the synthesis of 4-HIL. Therefore, in this section, Ile, α-KG, and O_2 supply as well as the conversion of Ile

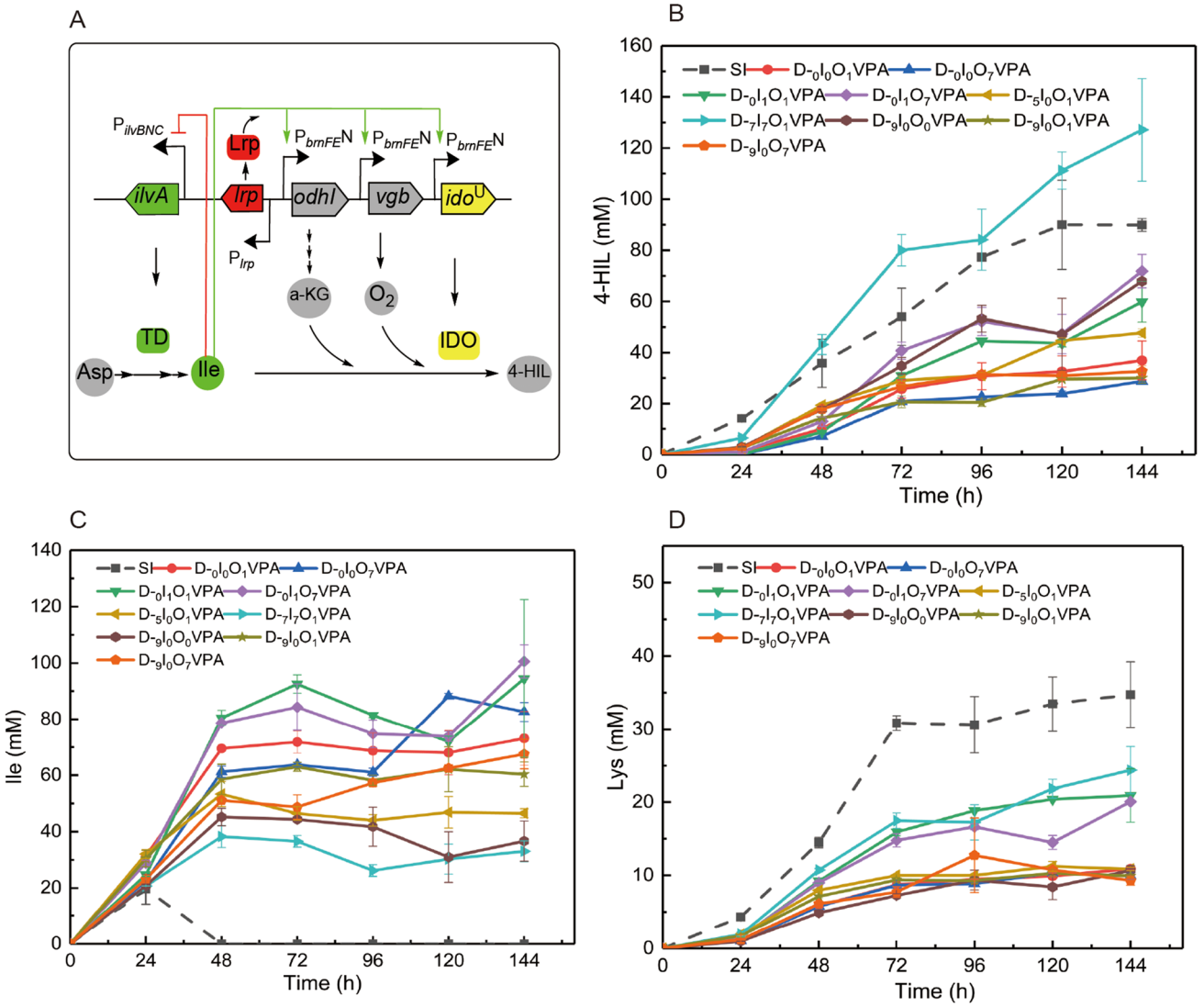

Fig. 5 Regulation circuit and 4-HIL fermentation of strains D-$_N$I$_N$O$_N$VPA. **A** Diagram of synergistic regulation circuit. Lrp-P_{brnFE}N positively regulated the expression of *ido*.^{U}, *odhI*, and *vgb* in response to intracellular Ile concentration, and P_{ilvBNC} negatively regulated the expression of *ilvA* in response to intracellular Ile concentration. **B** 4-HIL accumulation. **C** Ile accumulation. **D** The by-product Lys accumulation

to 4-HIL was synergistically controlled by upregulating the expression of *ido*^{U}, *odhI*, and *vgb* through Ile biosensor Lrp-P_{brnFE}N and downregulating the expression of *ilvA* through Ile attenuator P_{ilvBNC} (Fig. 5A). The P_{ilvBNC}-*ilvA* fragment was directly fused in the plasmids of above 12 strains for expression, and 9 D-$_{N}I_{N}O_{N}$VPA strains were obtained.

Eventually, D-$_{7}I_{7}O_{1}$VPA accumulated 127.1 ± 20.2 mM of 4-HIL, which was similar to the original strain D-$_{7}I_{7}O_{1}$V (131.2 ± 13.3 mM) and D-$_{7}$IPA (123.2 ± 20.5 mM). However, other strains generated much less 4-HIL than their original strains and SI (Fig. 5B). In these strains, the accumulation of Ile increased continuously in 48 h and then fluctuated thereafter. Finally, 40–90 mM of Ile was remained and not converted to 4-HIL (Fig. 5C). The above results showed that excessive Ile inhibited the enzyme activity of IDO and made Ile unable to convert into 4-HIL, resulting in low titer of 4-HIL. The concentration of Lys in these strains (9.3–26.4 mM) was slightly lower than D-$_{N}$IPA (16.1–31.8 mM) and SI (34.7 ± 4.5 mM) (Fig. 5D and 4E). In conclusion, except for D-$_{7}I_{7}O_{1}$VPA, the metabolic flow of other strains was redirected to the Ile or other by-products pathway, and simultaneous supply of Ile, α-KG, and O_2 failed to promote 4-HIL synthesis. Therefore, D-$_{7}I_{7}O_{1}$VPA in this section and D-$_{N}$IPA strains in the previous section are selected for further study.

Negative regulation of dapA expression and Lys synthesis by Lys-OFF riboswitch

A large amount of by-product Lys was accumulated in the above strains D-$_{N}$IPA. However, Lys is very important for cell growth. It is very difficult to eliminate Lys by gene knockout and other strategies (Yu et al. 2021). Therefore, in this section, a Lys OFF riboswitch was used to regulate the expression of *dapA*, the initial gene of Lys synthetic pathway, and thereby weaken the synthesis of Lys. When the Lys content increases, Lys can bind to the riboswitch to turn off the expression of *dapA* and weakens the synthesis of Lys. So that the concentration of Lys can be maintained at a level only necessary for cell growth (Fig. 6A). Therefore, the Lys-OFF riboswitch from *E. coli* MG1655 was integrated between the promoter and start codon of chromosomal *dapA* gene of SN01 to obtain the strain D-RS. Then, 7 dynamic regulatory plasmids of pIL-$_{N}I^{U}$PA and pIL-$_{7}I^{U}{}_{7}O_{1}$VPA were transformed into D-RS strain, generating strains of D-RS-$_{N}$IPA and D-RS-$_{7}I_{7}O_{1}$VPA.

During the whole fermentation process, the strain D-RS-$_{7}I_{7}O_{1}$VPA could not grow normally (data not shown). The strains D-RS-$_{1}$IPA and D-RS-$_{5}$IPA grew slightly slower, while the other D-RS-$_{N}$IPA strains grew similar to their corresponding D-$_{N}$IPA strains. Except the slightly slower rate of strain D-RS-$_{5}$IPA, the sugar consumption of other D-RS-$_{N}$IPA strains was similar to their corresponding D-$_{N}$IPA strains (Fig. 6B).

In D-RS-$_{5}$IPA, 4-HIL was synthesized steadily and continuously; finally, 177.3 ± 8.9 mM 4-HIL was accumulated (Fig. 6C). This titer was increased by 50.2% compared with D-$_{5}$IPA and increased by 97.2% compared with SI. Meanwhile, the concentration of Lys decreased to 6.1 ± 0.6 mM, which was 62.0% lower than D-$_{5}$IPA (Fig. 6E). Furthermore, this strain hardly produced other by-products (Fig. 6F). In D-RS-$_{D5}$IPA, the final titer of 4-HIL was similar to that of D-$_{D5}$IPA, but the concentration of Lys decreased to 6.8 mM, which was 74.0% lower than D-$_{D5}$IPA. And the Ile accumulation of these two strains was maintained at approximately 14 mM and 60 mM, respectively after 96 h (Fig. 6D). These results indicated that the regulation of *dapA* by Lys-OFF riboswitch weakened Lys synthesis without damaging the yield of 4-HIL in this two strains. While in D-RS-$_{0}$IPA and D-RS-$_{9}$IPA, although the concentration of Lys decreased greatly, the titer of 4-HIL also decreased by 17.6% and 28.6% compared with D-$_{0}$IPA and D-$_{9}$IPA, and these titers were even much lower than that of static strain SI (Fig. 6C, E). The above 4 strains grew rapidly but accumulated 4-HIL slowly in 0–48 h, while after 48 h, these strains grew slowly and accumulated 4-HIL rapidly (Fig. 6B, C), suggesting that the regulation of Lys synthesis by Lys-OFF riboswitch can provide basic Lys required for cell growth and thereby well balance the cell growth and 4-HIL synthesis. Strangely, in D-RS-$_{1}$IPA and D-RS-$_{7}$IPA strains, the production of 4-HIL and Ile was very low. However, a large amount of Lys was accumulated in D-RS-$_{1}$IPA (167.6 ± 4.6 mM) and D-RS-$_{7}$IPA (189.1 ± 4.9 mM) (Fig. 6C, E). The metabolic variation of these two strains will be studied in the future. In conclusion, the combined positive regulation of *ido* expression by Lrp-P_{brnFE}5 biosensor, negative regulation of *ilvA* expression by P_{ilvBNC} attenuator, and negative regulation of *dapA* expression by Lys-OFF riboswitch can better balance the metabolic flow and thereby promote the synthesis of 4-HIL and reduce the by-product Lys concentration greatly compared with other dynamic regulation strategies.

Discussion

Metabolic engineering faces many challenges. Competition for cell resources and sensitivity to fermentation conditions may lead to metabolic burden, imbalance of cofactors, or accumulation of metabolic intermediates to toxic levels, which will interfere with cell production and growth (Hartline et al. 2021). Dynamic metabolic engineering refers that the cell can independently regulate the expression of pathway, reroute metabolic flux, and guide the target metabolic pathway to solve the difficult problems in metabolic engineering, according to the changing intracellular and extracellular

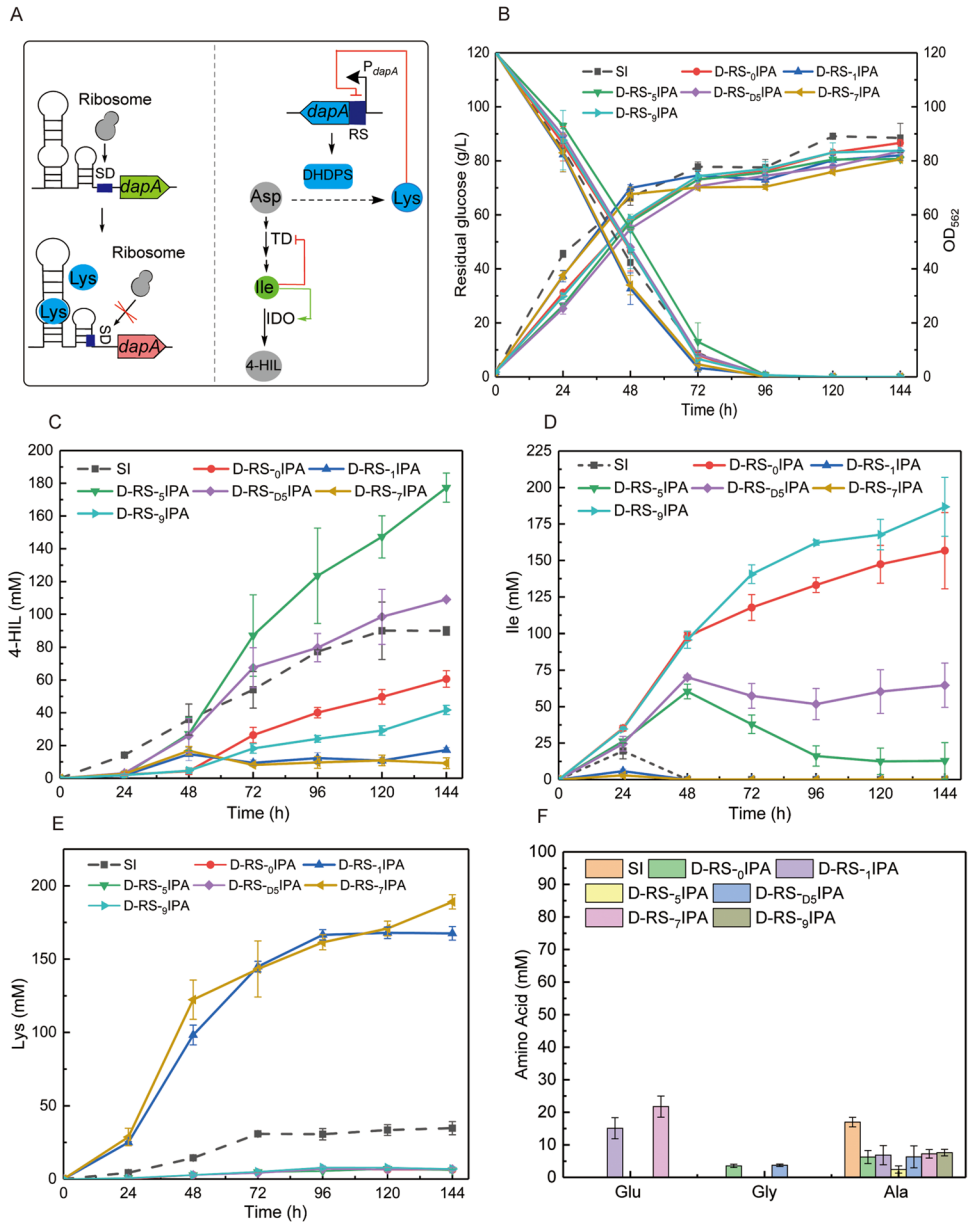

Fig. 6 Regulation circuit and 4-HIL fermentation of strains D-RS-$_N$IPA. **A** Circuit diagram regulated by Lys-OFF riboswitch. When Lys concentration is high, Lys combines with riboswitch to cause structural change of riboswitch. Then, this structure can prevent ribosomes from combining with SD region, thus turn off the transcription of *dapA*. **B** Cell growth and glucose consumption. **C** 4-HIL accumulation. **D** Ile accumulation. **E** The by-product Lys accumulation. **F** Other amino acid concentration at 144 h

environment (Brockman and Prather 2015). Dynamic control strategies include different kinds of switches or devices that can sense light, temperature, cell density, or some specific metabolites. Photogenetic switch can sense the visible light signal and make the responder undergo conformational changes and thereby regulate the expression of the target gene. In *E. coli*, a photosensor histidine kinase CcaS was used to respond to red light and green light to control the cell growth in the automatic photogenetic feedback control system (Milias-Argeitis et al. 2016). Similarly, a temperature-dependent system was used to dynamically regulate TCA cycle and thereby increase itaconate production in *E. coli* (Harder et al. 2018). In quorum sensing system, when the cell density exceeds a threshold, specific small molecules will accumulate and can be sensed to induce a specific reaction; thereby, this system can be used to dynamically balance cell growth and target yield (Tan and Prather 2017). For example, through regulating the response of cells to population signals at different cell densities, the conversion of *E. coli* from growth to production can be realized in different populations to improve the isopropanol yield (Soma and Hanai 2015). Metabolite-responsive biosensors usually sense specific metabolites to trigger conformational change of cognate actuator and regulate the expression of downstream genes. These biosensors can solve the problem of uncoordinated production and growth caused by the accumulation of intermediate metabolites, substrates, cofactors, and products. For example, Farmer et al. constructed a dynamic

control switch to regulate lycopene synthesis by using acetyl phosphate responsive TF-promoter (Farmer and Liao 2000). Zhou and Zeng used Lys-responsive riboswitch to regulate *gltA* expression and Lys synthesis (Zhou and Zeng 2015). The P_{ilvBNC} attenuator was used to weaken and regulate the expression of *icd* and *odhA*, thus increasing the production of Leu and 4-HIL, respectively (Luo et al. 2021; Zhang et al. 2018). There are fewer metabolite-responsive biosensors for metabolic engineering of *C. glutamicum.* Fortunately, both the upregulated and downregulated BCAAs-responsive biosensors have been found and explored, especially the Ile upregulated biosensors Lrp-P_{brnFE}N with different dynamic range (Tan et al. 2020). However, the Ile attenuator P_{ilvBNC} and Lys-OFF riboswitch were only preliminarily explored and they have not been applied cooperatively with other biosensors and verified thoroughly. Here, the Lrp-P_{brnFE}N and P_{ilvBNC} were applied coordinately to balance the upstream Ile synthesis and downstream Ile conversion pathways and to attenuate or avoid the substrate inhibition caused by excess Ile. The 4-HIL titer successfully increased to more than 120 mM (Fig. 4D, 5B). Most effectively, after synergistically downregulating Lys synthesis by Lys-OFF riboswitch, the 4-HIL titer increased greatly to more than 170 mM and the main by-product Lys content decreased greatly to about 6 mM (Fig. 6C). Therefore, the combined dynamic regulation of 4-HIL biosynthesis and Lys branch by these three biosensors can effectively promote 4-HIL biosynthesis in *C. glutamicum.*

4-HIL has potential value in the treatment of diabetes. In our previous study, 4-HIL was de novo synthesized from glucose by expressing the *ido* gene in *C. glutamicum* ssp. *lactofermentum* strain SN01, an Ile producer, and neither Ile nor α-KG was added (Shi et al. 2015). Therefore, the IDO activity is very important for the synthesis of 4-HIL. In the previous studies, the IDO activity was effectively improved by a series of static regulation methods, such as the directed evolution and site-specific mutation of *ido*, the coexpression of *ido* and *ido*3, and the ribosomal binding site (RBS) engineering of *ido* (Huang and Shi 2018; Shi et al. 2019, 2020). However, constitutive expression of *ido* may bring great metabolic burden to cells. Then, the Lrp-P_{brnFE}N biosensors were used to upregulate the expression of *ido* by sensing the intracellular Ile concentration. The yield of 4-HIL reached to 28.9 − 74.4 mM. However, 60 − 130 mM Ile was still accumulated and not converted into 4-HIL (Tan et al. 2020). In our study here, in order to further improve the IDO activity, the codon of *ido* was optimized and the Lrp-P_{brnFE}N biosensors were applied to upregulate the expression of ido^{U}. As expected, the yield of 4-HIL was further increased to 38.7 − 111.1 mM and the growth of the strains were not affected (Fig. 2B, C).

The coordinated supply of α-KG and O_2, the co-substrates of IDO reaction, is also very important for the synthesis of 4-HIL. In previous studies, to increase the supply of α-KG, the *aceA* gene (encoding isocitrate lyase of glyoxylate cycle) was deleted, thereby increasing the 4-HIL titer to 69.5 ± 2.2 mM (Shi et al. 2019). Then, strong promoters P_{dnaK} and P_{tacM} were used to statically control the expression of *vgb* on the basis of *aceA* deletion and *ido-mqo-ido*3 static expression. The yield of 4-HIL (91.2 mM and 88.0 mM) did not change significantly (Shi et al. 2019). Later, RBS with high, medium, and low intensities were used to statically fine-tune the expression of *odhI* on the basis of *ido* expression, and the yield of 4-HIL did not increase. Then RBS engineering was applied to fine-tune the expression of both *odhI* and *vgb* genes and the resulting supply of α-KG and O_2. The highest yield of 4-HIL was increased to 119.3 ± 5.0 mM (Shi et al. 2020). Subsequently, the natural and modified Lrp-P_{brnFE}N biosensors were used to dynamically upregulate the expression of *odhI* and *vgb*, and the highest yield of 4-HIL was increased to 135.3 ± 12.6 mM (Tan et al. 2020). Therefore, dynamic regulation may be more effective than static regulation in 4-HIL biosynthesis. In our study here, these three *lrp*-P_{brnFE}N biosensors with different strengths were utilized to coordinately upregulate the expression of *odhI* and *vgb*, and the highest yield of 4-HIL was increased to 141.1 ± 15.5 mM (Fig. 3). Previously, the natural Lrp-P_{brnFE} biosensor was used alone to dynamically regulate the expression of *odhI* and the resulting supply of α-KG, and the yield of 4-HIL was increased only by 8.3% (Zhang et al. 2018). Therefore, the modified Lrp-P_{brnFE}N biosensors with appropriate strength or dynamic range were more effective to regulate the supply of α-KG and O_2 and thereby enhanced the synthesis of 4-HIL significantly.

The synthesis of Ile and the conversion of Ile to 4-HIL need to be carefully balanced. In previous studies, constitutive expression of *ilvA*, *lysC*, or *POS5* led to excessive accumulation of Ile. However, the accumulated Ile could not be completely converted into 4-HIL and thus the 4-HIL titer decreased due to the inhibition of IDO activity by excessive Ile (Shi et al. 2016, 2018). Thereby, Ile supply shall be carefully modulated, but there is no research on the balanced Ile supply and 4-HIL synthesis. In our study here, Ile attenuator P_{ilvBNC} was used to dynamically control the synthesis of Ile and thus balance the upstream Ile supply and downstream Ile conversion pathways. The 4-HIL yield of one resulting bidirectional regulation strain D-$_7$IPA increased to 123.2 ± 20.5 mM (Fig. 4C). Therefore, bidirectional dynamic control of the Ile supply and conversion can effectively enhance the synthesis of 4-HIL. However, the dynamic range and threshold of Ile attenuator P_{ilvBNC} were not modified and only the natural P_{ilvBNC} was applied here. Moreover, in 9 D-$_N$I$_N$O$_N$VPA strains, 8 strains (except D-$_7$I$_7$O$_1$VPA) generated much less 4-HIL than their original high-producing D-$_N$I$_N$O$_N$V strains. It is speculated that in these high-producing D-$_N$I$_N$O$_N$VPA strains, the metabolic

flux has been well balanced, and the further expression of P_{ilvBNC}-controlled *ilvA* may destroy the existing balanced state of these strains. These results also indicate the fragility of metabolic balance and the necessity of dynamic regulation of 4-HIL synthesis. Even under the dynamic regulation manner, the upstream, downstream, and co-substrates supplying pathways should be optimized.

Lys is the main by-products in the synthesis of 4-HIL, but it is very important for the growth of cells (Wehrmann et al. 1998). In previous studies, a large amount of Lys was accumulated during the 4-HIL fermentation (Shi et al. 2019, 2020). Then, the strategy of programming adaptive laboratory evolution driven by Lys biosensor was exploited to weaken the synthesis of Lys, but the concentration of Lys did not decrease (Yu et al. 2021). In our study here, the Lys-OFF riboswitch was used to weaken Lys synthesis. The concentration of Lys successfully decreased to about 6 mM in most

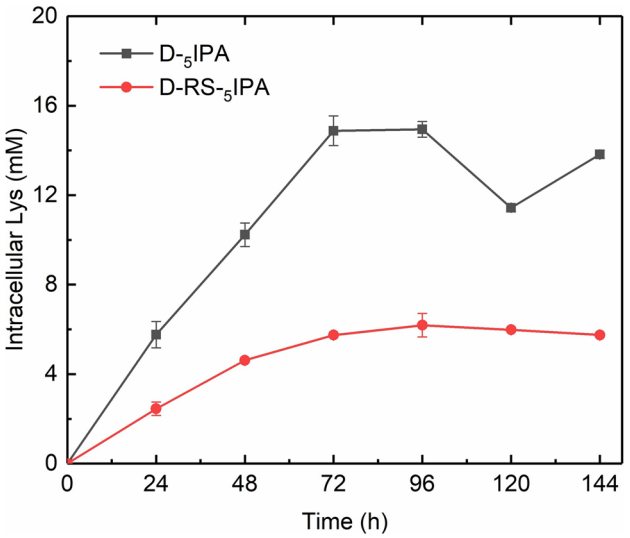

Fig. 7 The intracellular Lys accumulation in strains D-$_5$IPA and D-RS-$_5$IPA during 4-HIL fermentation

D-RS-$_N$IPA strains. Among them, the 4-HIL titer of D-RS-$_5$IPA strain (26.1 g/L) reached the highest level in shake flask fermentation according to current reports. However, there are still some shortcomings in this research. The sensitivity and basal expression of Lys-OFF riboswitch has not been optimized. The natural Lys-OFF riboswitch was reported to be very sensitive to Lys. It can strongly sense Lys low to 0.1 mM and thus directly turn off the synthesis of Lys (Zhou and Zeng 2015), but here, D-RS-$_N$IPA strains could accumulate up to 6 mM Lys. Thereupon, the intracellular accumulation of Lys in D-$_5$IPA and D-RS-$_5$IPA was determined. As shown in Fig. 7, the intracellular Lys content of D-$_5$IPA and D-RS-$_5$IPA was 10–15 mM and 5–6 mM, respectively, similar to their extracellular Lys content. This content was much higher than the reported threshold of Lys-OFF riboswitch. Such discrepancy may be caused by the differences between our engineering strain derived from *C. glutamicum* SN01 and the strain *C. glutamicum* ATCC 13,032 used by Zhou and Zeng (2015). However, we failed to characterize the response of Lys-OFF riboswitch to Lys and determine its threshold in our engineering strain by fluorescence assay, because our engineering strain could not grow in Lys restricted medium at all. In addition, Lys-OFF riboswitch cannot gradually downregulate gene expression and Lys synthesis. However, prematurely turning off the Lys synthesis will affect cell growth. Therefore, the modified Lys-OFF riboswitch with higher threshold still needs to be exploited in the future. A recent review also suggests that fine-tuning biosensors is required to adjust the threshold concentrations required to switch a TF or riboswitch to the requirements of strain development (Wendisch 2020). Here, the 4-HIL titer of the best strain D-RS-$_5$IPA (26.1 g/L) is 51.7% and 26.7% higher than that of previously reported static control strains SZ05^{opt} (17.2 g/L) (Shi et al. 2019) and SF12 (20.6 g/L) (Shi et al. 2020), respectively (Table 3). This titer is also 31.2% higher than that of previously reported dynamic control strain ST17 regulated by single-functional biosensor (19.9 g/L) (Tan et al. 2020). Therefore, multi-functional

Table 3 4-HIL productions in recombinant *C. glutamicum* strains

Strains		4-HIL titer (g/L)	Lys content (mM)	Glucose consumption (g/L)	4-HIL yield from glucose (mol/mol)	4-HIL productivity [g/(L•h)]	Ile to 4-HIL conversion ratio (mol/mol)	References
HIL18	Fermenter	34.2	≈4.0	228.4	0.150	0.535	0.98	Zhang et al. 2018
	Flask	6.2	≈0.3	42.5	0.179	0.128	0.98	
SZ05^{opt}	Flask	17.2	≈25.0	127.0	0.166	0.120	1.00	Shi et al. 2019
SF12	Flask	20.6	≈30.0	127.0	0.198	0.143	0.94	Shi et al. 2020
ST17	Flask	19.9	≈20.0	127.0	0.186	0.138	0.88	Tan et al. 2020
D-$_0$I$_7$O$_7$V	Flask	20.7	—	127.0	0.199	0.144	—	This work
D-$_7$I$_7$O$_1$V	Flask	19.5	—	127.0	0.187	0.135	—	This work
D-RS-$_5$IPA	Flask	26.1	6.1	127.0	0.251	0.181	0.93	This work

dynamic control system would be more effective for 4-HIL biosynthesis than static metabolic engineering and single functional dynamic control system. D-RS-$_5$IPA is a promising candidate for producing 4-HIL. However, its 4-HIL titer in shake flasks was lower than that of HIL18 achieved by 7 steps of static and 1 step of dynamic metabolic engineering in the bioreactor (34.2 g/L) (Zhang et al. 2018). The fed-batch fermentation of D-RS-$_5$IPA will be considered in the future.

Author contribution FS conceived and designed the research. WL, ST, HL, and YX conducted the experiments. WL, FS, and ST analyzed the data. FS, WL, and YL wrote the manuscript. All authors read and approved the manuscript.

Funding This work was supported by the program of State Key Laboratory of Food Science and Technology (SKLF-ZZA-201904).

Data availability The data used to support the findings of this study are available from the corresponding author upon request.

Declarations

Ethics approval and consent to participate This article does not contain any studies with human participants or animals performed by any of the authors.

Conflict of interest The authors declare no competing interests.

References

Anesiadis N, Cluett WR, Mahadevan R (2008) Dynamic metabolic engineering for increasing bioprocess productivity. Metab Eng 10(5):255–266. https://doi.org/10.1016/j.ymben.2008.06.004

Becker J, Rohles CM, Wittmann C (2018) Metabolically engineered *Corynebacterium glutamicum* for bio-based production of chemicals, fuels, materials, and healthcare products. Metab Eng 50:122–141. https://doi.org/10.1016/j.ymben.2018.07.008

Brockman IM, Prather KLJ (2015) Dynamic metabolic engineering: New strategies for developing responsive cell factories. Biotechnol J 10(9):1360–1369. https://doi.org/10.1002/biot.201400422

Farmer WR, Liao JC (2000) Improving lycopene production in *Escherichia coli* by engineering metabolic control. Nat Biotechnol 18(5):533–537. https://doi.org/10.1038/75398

Harder BJ, Bettenbrock K, Klamt S (2018) Temperature-dependent dynamic control of the TCA cycle increases volumetric productivity of itaconic acid production by *Escherichia coli*. Biotechnol Bioeng 115:156–164. https://doi.org/10.1002/bit.26446

Hartline CJ, Schmitz AC, Han Y, Zhang F (2021) Dynamic control in metabolic engineering: theories, tools, and applications. Metab Eng 63:126–140. https://doi.org/10.1016/j.ymben.2020.08.015

Holtz WJ, Keasling JD (2010) Engineering static and dynamic control of synthetic pathways. Cell 140(1):19–23. https://doi.org/10.1016/j.cell.2009.12.029

Hu J, Li Y, Zhang H, Tan Y, Wang X (2014) Construction of a novel expression system for use in *Corynebacterium glutamicum*. Plasmid 75:18–26. https://doi.org/10.1016/j.plasmid.2014.07.005

Huang S, Shi F (2018) Directed evolution and site-specific mutagenesis of L-isoleucine dioxygenase derived from *Bacillus weihenstephanensis*. Biotechnol Lett 40(8):1227–1235. https://doi.org/10.1007/s10529-018-2566-8

Jin LQ, Jin WR, Ma ZC, Shen Q, Cai X, Liu ZQ, Zheng YG (2019) Promoter engineering strategies for the overproduction of valuable metabolites in microbes. Appl Microbiol Biotechnol 103(21–22):8725–8736. https://doi.org/10.1007/s00253-019-10172-y

Jones KL, Kim SW, Keasling JD (2000) Low-copy plasmids can perform as well as or better than high-copy plasmids for metabolic engineering of bacteria. Metab Eng 2(4):328–338. https://doi.org/10.1006/mben.2000.0161

Jones CM, Hernández Lozada NJ, Pfleger BF (2015) Efflux systems in bacteria and their metabolic engineering applications. Appl Microbiol Biotechnol 99(22):9381–9393. https://doi.org/10.1007/s00253-015-6963-9

Kortmann M, Mack C, Baumgart M, Bott M (2019) Pyruvate carboxylase variants enabling improved Lysine production from glucose identified by biosensor-based high-throughput fluorescence-activated cell sorting screening. ACS Synth Biol 8(2):274–281. https://doi.org/10.1021/acssynbio.8b00510

Liu Y, Shin HD, Li J, Liu L (2015) Toward metabolic engineering in the context of system biology and synthetic biology: advances and prospects. Appl Microbiol Biotechnol 99(3):1109–1118. https://doi.org/10.1007/s00253-014-6298-y

Liu C, Zhang B, Liu YM, Yang KQ, Liu SJ (2018) New intracellular shikimic acid biosensor for monitoring shikimate synthesis in *Corynebacterium glutamicum*. ACS Synth Biol 7(2):591–601. https://doi.org/10.1021/acssynbio.7b00339

Liu H, Shi F, Tan S, Yu X, Lai W, Li Y (2021) Engineering a bifunctional ComQXPA-P$_{srfA}$ quorum-sensing circuit for dynamic control of gene expression in *Corynebacterium glutamicum*. ACS Synth Biol 10(7):1761–1774. https://doi.org/10.1021/acssynbio.1c00149

Luo G, Zhao N, Jiang S, Zheng S (2021) Application of RecET-Cre/loxP system in *Corynebacterium glutamicum* ATCC14067 for L-leucine production. Biotechnol Lett 43(1):297–306. https://doi.org/10.1007/s10529-020-03000-1

Milias-Argeitis A, Rullan M, Aoki SK, Buchmann P, Khammash M (2016) Automated optogenetic feedback control for precise and robust regulation of gene expression and cell growth. Nat Commun 7:12546. https://doi.org/10.1038/ncomms12546

Morbach S, Junger C, Sahm H, Eggeling L (2000) Attenuation gontrol of *ilvBNC* in *Corynebacterium glutamicum*: evidence of leader peptide formation without the presence of a ribosome binding site. J Biosci Bioeng 90(5):501–507. https://doi.org/10.1016/S1389-1723(01)80030-X

Mustafi N, Grünberger A, Kohlheyer D, Bott M, Frunzke J (2012) The development and application of a single-cell biosensor for the detection of L-methionine and branched-chain amino acids. Metab Eng 14(4):449–457. https://doi.org/10.1016/j.ymben.2012.02.002

Nielsen J, Keasling JD (2016) Engineering cellular metabolism. Cell 164(6):1185–1197. https://doi.org/10.1016/j.cell.2016.02.004

Nowroozi FF, Baidoo EE, Ermakov S, Redding-Johanson AM, Batth TS, Petzold CJ, Keasling JD (2014) Metabolic pathway optimization using ribosome binding site variants and combinatorial gene assembly. Appl Microbiol Biotechnol 98(4):1567–1581. https://doi.org/10.1007/s00253-013-5361-4

Renicke C, Taxis C (2016) Biophotography: concepts, applications and perspectives. Appl Microbiol Biotechnol 100(8):3415–3420. https://doi.org/10.1007/s00253-016-7384-0

Salis HM, Mirsky EA, Voigt CA (2009) Automated design of synthetic ribosome binding sites to control protein expression. Nat Biotechnol 27(10):946–950. https://doi.org/10.1038/nbt.1568

Schäfer A, Tauch A, Jäger W, Kalinowski J, Thierbach G, Pühler A (1994) Small mobilizable multi-purpose cloning vectors derived

from the *Escherichia coli* plasmids pK18 and pK19: selection of defined deletions in the chromosome of *Corynebacterium glutamicum*. Gene 145(1):69–73. https://doi.org/10.1016/0378-1119(94)90324-7

Shi F, Niu T, Fang H (2015) 4-Hydroxyisoleucine production of recombinant Corynebacterium glutamicum ssp lactofermentum under optimal corn steep liquor limitation. Appl Microbiol Biotechnol 99(9):3851–3863. https://doi.org/10.1007/s00253-015-6481-9

Shi F, Fang H, Niu T, Lu Z (2016) Overexpression of *ppc* and *lysC* to improve the production of 4-hydroxyisoleucine and its precursor L-isoleucine in recombinant *Corynebacterium glutamicum* ssp. *lactofermentum*. Enzyme Microb Technol 87–88:79–85. https://doi.org/10.1016/j.enzmictec.2016.04.008

Shi F, Zhang M, Li Y, Fang H (2018) Sufficient NADPH supply and *pknG* deletion improve 4-hydroxyisoleucine production in recombinant *Corynebacterium glutamicum*. Enzyme Microb Technol 115:1–8. https://doi.org/10.1016/j.enzmictec.2018.04.003

Shi F, Zhang S, Li Y, Lu Z (2019) Enhancement of substrate supply and ido expression to improve 4-hydroxyisoleucine production in recombinant Corynebacterium glutamicum ssp lactofermentum. Appl Microbiol Biotechnol 103(10):4113–4124. https://doi.org/10.1007/s00253-019-09791-2

Shi F, Fan Z, Zhang S, Wang Y, Tan S, Li Y (2020) Optimization of ribosomal binding site sequences for gene expression and 4-hydroxyisoleucine biosynthesis in recombinant *corynebacteriumglutamicum*. Enzyme Microb Technol 140:109622. https://doi.org/10.1016/j.enzmictec.2020.109622

Smirnov SV, Kodera T, Samsonova NN, Kotlyarova VA, Rushkevich NY, Kivero AD, Sokolov PM, Hibi M, Ogawa J, Shimizu S (2010) Metabolic engineering of *Escherichia coli* to produce (2S, 3R, 4S)-4-hydroxyisoleucine. Appl Microbiol Biotechnol 88(3):719–726. https://doi.org/10.1007/s00253-010-2772-3

Soma Y, Hanai T (2015) Self-induced metabolic state switching by a tunable cell density sensor for microbial isopropanol production. Metab Eng 30:7–15. https://doi.org/10.1016/j.ymben.2015.04.005

Tan SZ, Prather KL (2017) Dynamic pathway regulation: recent advances and methods of construction. Curr Opin Chem Biol 41:28–35. https://doi.org/10.1016/j.cbpa.2017.10.004

Tan S, Shi F, Liu H, Yu X, Wei S, Fan Z, Li Y (2020) Dynamic control of 4-hydroxyisoleucine biosynthesis by modified L-isoleucine biosensor in recombinant *Corynebacterium glutamicum*. ACS Synth Biol 9(9):2378–2389. https://doi.org/10.1021/acssynbio.0c00127

Venayak N, Anesiadis N, Cluett WR, Mahadevan R (2015) Engineering metabolism through dynamic control. Curr Opin Biotechnol 34:142–152. https://doi.org/10.1016/j.copbio.2014.12.022

Wehrmann A, Phillipp B, Sahm H, Eggeling L (1998) Different modes of diaminopimelate synthesis and their role in cell wall integrity: a study with *Corynebacterium glutamicum*. J Bacteriol 180(12):3159–3165. https://doi.org/10.1128/JB.180.12.3159-3165.1998

Wendisch VF (2020) Metabolic engineering advances and prospects for amino acid production. Metab Eng 58:17–34. https://doi.org/10.1016/j.ymben.2019.03.008

Winkler WC, Breaker RR (2005) Regulation of bacterial gene expression by riboswitches. Annu Rev Microbiol 59:487–517. https://doi.org/10.1146/annurev.micro.59.030804.121336

Yang Y, Lin Y, Wang J, Wu Y, Zhang R, Cheng M, Shen X, Wang J, Chen Z, Li C, Yuan Q, Yan Y (2018) Sensor-regulator and RNAi based bifunctional dynamic control network for engineered microbial synthesis. Nat Commun 9(1):3043. https://doi.org/10.1038/s41467-018-05466-0

Yang J, Ran Y, Yang Y, Song S, Wu Y, Qi Y, Gao Y, Li G (2020) 4-Hydroxyisoleucine alleviates macrophage-related chronic inflammation and metabolic syndrome in mice fed a high-fat diet. Front Pharmacol 11:606514. https://doi.org/10.3389/fphar.2020.606514

Yu X, Shi F, Liu H, Tan S, Li Y (2021) Programming adaptive laboratory evolution of 4-hydroxyisoleucine production driven by a lysine biosensor in *Corynebacterium glutamicum*. AMB Express 11(1):66. https://doi.org/10.1186/s13568-021-01227-3

Zafar MI, Gao F (2016) 4-Hydroxyisoleucine: a potential new treatment for type 2 diabetes mellitus. BioDrugs 30(4):255–262. https://doi.org/10.1007/s40259-016-0177-2

Zhang F, Carothers JM, Keasling JD (2012) Design of a dynamic sensor-regulator system for production of chemicals and fuels derived from fatty acids. Nat Biotechnol 30(4):354–359. https://doi.org/10.1038/nbt.2149

Zhang C, Li Y, Ma J, Liu Y, He J, Li Y, Zhu F, Meng J, Zhan J, Li Z, Zhao L, Ma Q, Fan X, Xu Q, Xie X, Chen N (2018) High production of 4-hydroxyisoleucine in *Corynebacterium glutamicum* by multistep metabolic engineering. Metab Eng 49:287–298. https://doi.org/10.1016/j.ymben.2018.09.008

Zhou LB, Zeng AP (2015) Exploring lysine riboswitch for metabolic flux control and improvement of L-lysine synthesis in *Corynebacterium glutamicum*. ACS Synth Biol 4(6):729–734. https://doi.org/10.1021/sb500332c

Zhou P, Xie W, Yao Z, Zhu Y, Ye L, Yu H (2018) Development of a temperature-responsive yeast cell factory using engineered Gal4 as a protein switch. Biotechnol Bioeng 115(2):1321–1330. https://doi.org/10.1002/bit.26544

Zhou L, Ren J, Li Z, Nie J, Wang C, Zeng AP (2019) Characterization and engineering of a clostridium glycine riboswitch and its use to control a novel metabolic pathway for 5-aminolevulinic acid production in *Escherichia coli*. ACS Synth Biol 8(10):2327–2335. https://doi.org/10.1021/acssynbio.9b00137